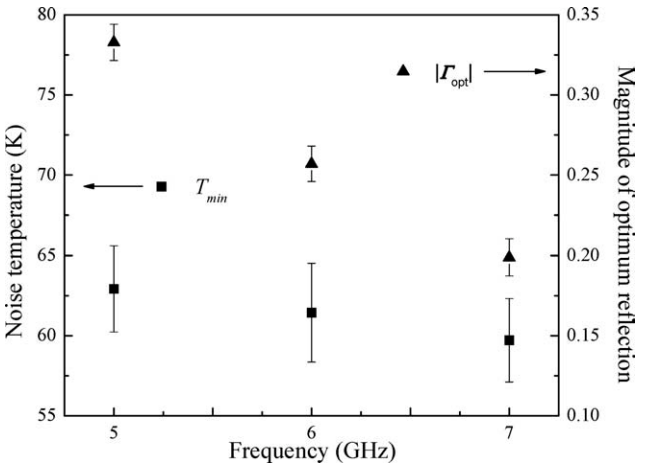

Figure 4 Fitted results of LNA T_{min} and LNA $|\Gamma_{opt}|$ from five day VTU measurements. Error bars indicate the standard uncertainty (1σ)

program. Type-B uncertainty is evaluated through a Monte Carlo simulation program [5]. The uncertainties in T_{min} at all frequencies are below 5.1%, and the uncertainties in $|\Gamma_{opt}|$ are below 5.8%. The fitted reduced gain is within 0.065 dB difference from the values measured on the VNA (~32.4 dB) at all three frequency points. These results are comparable to the previous VTU measurements [2].

5. DISCUSSION AND CONCLUSIONS

Here, we want to emphasize that we have not exercised intensive efforts in the design of a high-end component. Rather, the goal of this article is to demonstrate, for the first time, an efficient noise-parameter de-embedding method by use of a simplified phase shifter. In comparison to commercially available solid-state tuners based on PIN-diode arrays, the phase shifter consisting of varactors is a continuous impedance synthesizer, requiring fewer numbers of components to provide the same number of impedance states. Furthermore, PIN-diodes at fully on state draw non-negligible currents and contribute shot noise in addition to thermal noise [6]. For precision measurement purpose, they can be no longer considered as passive devices and need extra step to characterize their noise emission.

However, the prototype phase shifter used for noise-parameter measurements does need improvements. It has limited bandwidth and its reflection magnitude is not variable. First, a broadband coupler can be designed by means of a multi-layer microstrip circuit [7], although that increases the complexity in fabrication and packaging. Second, the reflection magnitude can be increased by improving the microstrip-to-coaxial coupling. Moreover, the parasitic resistance of the varactor can be compensated by adding a bipolar junction transistor (BJT) in series, which has negative resistance characteristic [8]. Third, rather than leaving it unconnected, we can terminate the isolation port of the coupler with a junction field-effect transistor (JFET), functioning as a voltage controlled resistor (VCR). Therefore, the magnitude of the reflection will be also adjustable, which in turn creates more mapping capability on the Smith chart.

In conclusion, we have successfully demonstrated the design, fabrication, and implementation of a 5–7 GHz phase shifter for noise-parameter extraction on a packaged amplifier. The phase shifter provides ultra-portability and fast response, far better than a mechanical tuner. Its good repeatability ensures the direct use on noise temperature instruments without online VNA requirement. The measured results showed acceptable uncertainty. We also expect that the design is compatible with the transistor fabrication process and can potentially be incorporated onto the same wafer to provide quick on-wafer metrology.

REFERENCES

1. C.E. Woodin and D.L. Wandrei, High power solid state programmable load, U.S. Patent 5,276,411 (1994).
2. D. Gu, D.K. Walker, and J. Randa, Variable termination unit for noise parameter measurement, IEEE Trans Instrum Meas 58 (2008), 1072–1077.
3. C.A. Grosvenor, J. Randa, and R.L. Billinger, Design and testing of NFRad—A new noise measurement system, NIST Technical Note, TN1518, NIST, Boulder, CO (2000).
4. J. Randa and D.K. Walker, Amplifer noise-parameter measurement checks and verification, Presented at the 63rd ARFTG Conference Digest, Fort Worth, TX (2004), pp. 41–45.
5. J. Randa, Uncertainty analysis for noise-parameter measurements at NIST, IEEE Trans Instrum Meas 58 (2009) 1146–1151.
6. M. Jankovec, H. Stiebig, F. Smole, and M. Topic, Noise characterization of a-Si:H pin diodes, J Non Cryst Solids 352 (2006), 1829–1831.
7. A.M. Abbosh and M.E. Bialkowski, Design of compact directional couplers for UWB applications, IEEE Trans Microwave Theory Tech 55 (2007), 189–194.
8. K.T. Park, Y.H. Cho, and S.W. Yun, Low voltage tunable narrow bandpass filter using cross-coupled stepped-impedance resonator with active capacitance circuit, IEEE MTTS Int Microwave Symp Dig, Boston, MA (2009), 1049–1052.

SMALL-SIZE 11-BAND LTE/WWAN/WLAN INTERNAL MOBILE PHONE ANTENNA

Shu-Chuan Chen and Kin-Lu Wong
Department of Electrical Engineering National Sun Yat-sen University, Kaohsiung 80424, Taiwan; Corresponding author: wongkl@ema.ee.nsysu.edu.tw

Received 13 February 2010

ABSTRACT: *This work presents an internal mobile phone antenna occupying a small board space of 600 mm^2 on the system circuit board and providing three wide operating bands of at least 698–960, 1710–2690, and 5150–5825 MHz for the 11-band long term evolution (LTE)/wireless wide area network (WWAN)/wideband local area network (WLAN) operation. This includes three LTE bands of LTE700/2300/2500, five WWAN bands of GSM850/900/1800/1900/UMTS, and three WLAN 2.4/5.2/5.8 GHz bands. The antenna is a coupled-fed shorted monopole, with a wide feeding strip in the coupling feed, a long shorting strip closely coupled to the shorted monopole, and a tuning stub connected to the shorting strip. The antenna's three wide operating bands are achieved and controlled by tuning the width of the feeding strip, the gap between the shorting strip and the shorted monopole, and the dimensions of the tuning stub. Operating principle of the proposed antenna is described in detail in this article. Results of the fabricated antenna are presented and discussed. The specific absorption rate results of the antenna with the presence of the user's head and hand are also studied.* © 2010 Wiley Periodicals, Inc. Microwave Opt Technol Lett 52:2603–2608, 2010; View this article online at wileyonlinelibrary.com. DOI 10.1002/mop.25526

Key words: *mobile antennas; handset antennas; LTE antennas; WWAN antennas; WLAN antennas*

1. INTRODUCTION

To achieve small size and wideband operation is generally demanded for the internal mobile phone antennas [1]. This is a

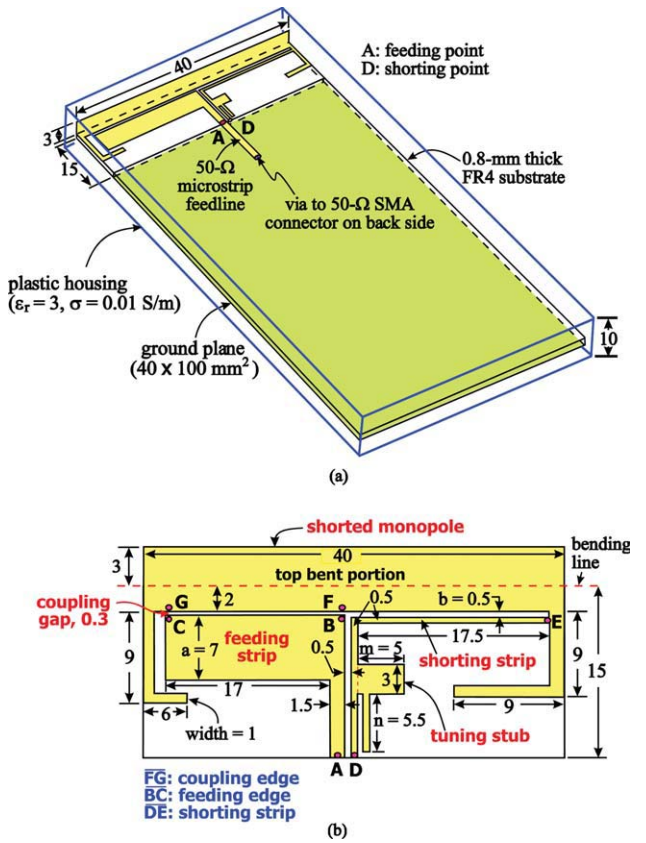

Figure 1 (a) Geometry of the proposed small-size 11-band LTE/WWAN/WLAN internal mobile phone antenna. (b) Dimensions of the antenna. [Color figure can be viewed in the online issue, which is available at wileyonlinelibrary.com]

major challenging design issue for the internal wireless wide area network (WWAN) antenna, especially in its applications in the slim mobile phones in which the internal antenna should have a thin profile (generally less than 4 mm) [2–6]. For achieving WWAN operation in the five operating bands of GSM850/900/1800/1900/UMTS (824–894/880–960/1710–1880/1850–1990/1920–2170 MHz), some promising on-board printed antennas have been reported in the published articles [7–14], in which the antenna generally requires a small board space of about 600 mm^2 or less and is suitable for slim mobile phone applications. Recently, promising thin-profile internal mobile phone antenna designs for achieving the 8-band operation for WWAN and long term evolution (LTE [15]) operation have also been reported [16], in which the antenna can provide two wide operating bands of 698–960 and 1710–2690 MHz for the 8-band LTE/WWAN operation.

In this work, we push the limit of the thin-profile internal mobile phone antenna with a small size to cover the 11-band operation which includes three LTE bands of LTE700/2300/2500 (698–787/2300–2400/2500–2690 MHz), five WWAN bands of GSM850/900/1800/1900/UMTS, and three WLAN 2.4/5.2/5.8 GHz bands (2400–2484/ 5150–5350/5725–5825 MHz). For the 11-band operation, the proposed antenna in the article occupies a small board space of 600 mm^2 on the system circuit board of the mobile phone and provides three wide operating bands of at least 698–960, 1710–2690, and 5150–5825 MHz. For the LTE and WWAN bands, the impedance matching for frequencies over the bands is better than 6-dB return loss, while for the wideband local area network (WLAN) bands, the impedance matching over the bands is better than 10-dB return loss.

The proposed antenna is a coupled-fed shorted monopole. The small-size wideband operation is obtained by using a wide feeding strip in the coupling feed, a long shorting strip closely coupled to the shorted monopole, and a tuning stub connected to the shorting strip. Detailed dimensions of the proposed antenna are described, and the operating principle for small-size wideband operation is discussed in the article. The antenna was also fabricated and tested, and results of the fabricated antenna are presented. The radiation characteristics of the antenna including the specific absorption rate (SAR) [17–19] values for the 1-g tissue of the head only and the head and hand are also analyzed.

2. PROPOSED ANTENNA

Figure 1(a) shows the geometry of the proposed antenna, whose detailed dimensions are given in Figure 1(b). The antenna is a coupled-fed shorted monopole and is disposed on the board space of size 15 $\times$ 40 mm^2 on the system circuit board of the mobile phone. The antenna mainly comprises a shorted monopole, a wide feeding strip to capacitively excite the shorted monopole, a long shorting strip (section DE) with a large portion closely coupled to the shorted monopole, and a tuning stub connected to shorting strip. The metal pattern of the antenna is mainly printed on the system circuit board, except that a top bent portion made from a 0.2-mm thick metal plate is connected to the shorted monopole. This top bent portion is chosen to have a width of 3 mm such that it can fit in the modern slim mobile phone with a thin profile, and it can help in achieving good radiation efficiency of the antenna, especially the radiating frequency at the lower frequencies in the LTE700/GSM850/900 bands.

In the study, the system circuit board is made from a 0.8-mm thick FR4 substrate of relative permittivity 4.4 and loss tangent 0.024. On the back side of the FR4 substrate, a ground plane of width 40 mm and length 100 mm is printed, which is treated as the system ground plane of the mobile phone. A plastic housing made from 1-mm thick plastic slab of relative permittivity 3.0 and conductivity 0.01 S/m encloses the FR4 substrate as the mobile phone housing. The plastic housing is chosen to have a thickness of 10 mm in the study, and the system circuit board is arranged to be at about the center of the plastic housing.

The antenna can provide three wide operating bands; the first band covers the LTE700/GSM850/900 (698–960 MHz) with return loss better than 6 dB, the second band covers the GSM1800/1900/UMTS (1710–2690 MHz) with return loss better than 6 dB and the 2.4 GHz WLAN (2400–2484 MHz) with return loss better than 10 dB, and the third band covers the 5.2/5.8 GHz WLAN (5150–5825 MHz) with return loss better than 10 dB. To achieve good impedance matching for frequencies over the first band, the long shorting strip in the proposed antenna is crucial. With a large portion of the shorting strip closely coupled to the shorted monopole with a small gap (b) of 0.5 mm, it helps achieve improved impedance matching over the first band. For the second band, the wide feeding strip with a width (a) of 7 mm is effectively in achieving good impedance matching for frequencies over the second band, especially those over the 2.4 GHz WLAN band. This is because the wide feeding strip has a resonant length close to 0.25-wavelength of the frequencies in the second band, hence the widened width of the feeding strip is especially helpful in improving the impedance matching in the second band.

For the third band, the tuning stub connected to the shorting strip is crucial. As shown in the figure, the tuning stub is of an asymmetric T-shape. By adjusting the length m and n (selected

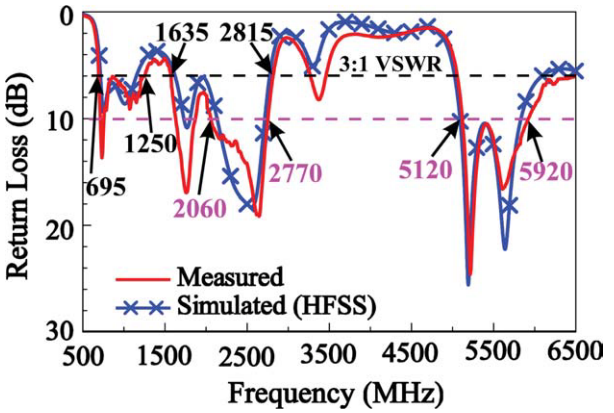

Figure 2 Measured and simulated return loss for the fabricated antenna. [Color figure can be viewed in the online issue, which is available at wileyonlinelibrary.com]

to be 5.0 and 5.5 mm in the study, respectively), the impedance matching for frequencies in the third band can be greatly improved to achieve good impedance matching better than 10 dB in return loss.

Also notice that the shorted monopole is generally formed into a C-shape, such that it can provide a resonant length of about 80 mm, although the width of the system circuit board is 40 mm only in the study. This resonant length is close to 0.25-wavelength of the frequencies in the first band, hence the shorted monopole can support the excitation of the resonant modes for the first band. The shorted monopole is excited capacitively by the feeding strip through a coupling gap of 0.3 mm between the feeding edge (section BC) in the feeding strip and the coupling edge (section FG) in the shorted monopole. With the coupling feed, it is promising for the shorted monopole to achieve dual-resonance excitation for the excited quarter-wavelength resonant mode such that the wideband operation for the antenna's first band can be obtained. The operating principle of the coupling-feed mechanism in achieving the dual-resonance excitation for the excited resonant mode for the coupled-fed PIFAs (planar inverted-F antennas) or shorted monopoles has also been recently studied [20–24]; however, in the recent studies, the obtained bandwidths of the excited dual-resonant mode can cover the GSM850/900 (824–960 MHz) operation only.

3. RESULTS AND DISCUSSION

The proposed antenna was fabricated and experimentally studied. Figure 2 shows the measured and simulated return loss for the fabricated antenna. The simulation results are obtained using Ansoft simulation software HFSS version 12 [25]. The measured data are observed to agree with the simulated results. From the results, three wide operating bands have been obtained for the antenna. The first band has a very wide 3-dB return-loss bandwidth of 555 MHz (695–1250 MHz), which easily covers the LTE700/GSM850/900 operation. Note that the 6-dB return loss (3:1 VSWR) is widely used as the internal mobile phone antenna design specification for the LTE/WWAN operation. The second band also shows a very wide 6-dB return-loss bandwidth of 1180 MHz (1635–2815 MHz), allowing the antenna to cover the GSM1800/1900/UMTS/LTE2300/2500 operation. Also, for the 10-dB return-loss bandwidth generally required for the WLAN operation, the second band provides a bandwidth of 710 MHz (2060–2770 MHz), wide enough to cover the 2.4 GHz WLAN operation. For the third band, it has a wide 10-dB return-loss bandwidth of 800 MHz (5120–5920 MHz), which covers the 5.2/5.8 GHz WLAN operation. Hence, from the obtained results, the 11-band LTE/WWAN/WLAN operation is obtained for the proposed antenna.

The operating principle of the proposed antenna is analyzed in Figure 3, in which the simulated return-loss results for the proposed antenna, the case with a simple feeding strip and a simple shorting strip (Ref1), Ref1 with a long shorting strip coupled to the shorted monopole (Ref2), Ref2 with a widened feeding strip (Ref3), and Ref3 with a simple tuning stub connected to the shorting strip (Ref4) are presented. All the corresponding dimensions of the five antennas studied in the figure are the same. Ref1 uses a simple coupling feed and a simple shorting strip for the shorted monopole; three resonant modes at about 1300, 1900, and 5000 MHz are excited; however, the obtained bandwidths are far from covering the required operating bands. By modifying Ref1 to introduce a long shorting strip with a large portion closely coupled to the shorted monopole (Ref2), dual-resonance excitation of the resonant mode in the desired first band is obtained; however, the other two resonant modes at about 1900 and 5000 MHz are relatively slightly affected by the introduced long shorting strip.

Further, by widening the feeding strip as seen for Ref3, a very wide second band is obtained. This is achieved by an additional resonant mode at about 2400 MHz, which incorporates the resonant mode at about 1900 MHz to form the desired second band. This additional new resonant mode is contributed by the widened feeding strip as explained in Section 2. For Ref3,

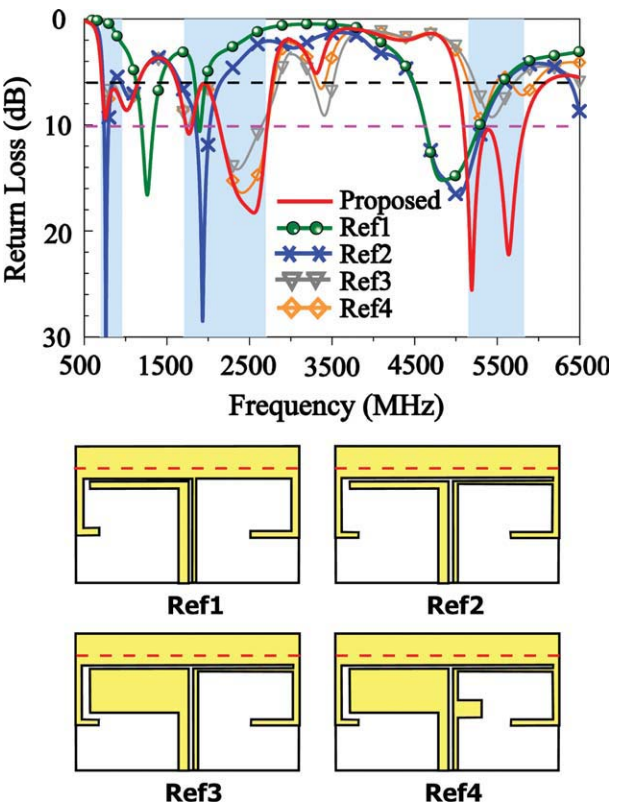

Figure 3 Simulated return loss for the proposed antenna, the case with a simple feeding strip and a simple shorting strip (Ref1), Ref1 with a long shorting strip closely coupled to the shorted monopole (Ref2), Ref2 with a widened feeding strip (Ref3), and Ref3 with a simple tuning stub connected to the shorting strip (Ref4). [Color figure can be viewed in the online issue, which is available at wileyonlinelibrary.com]

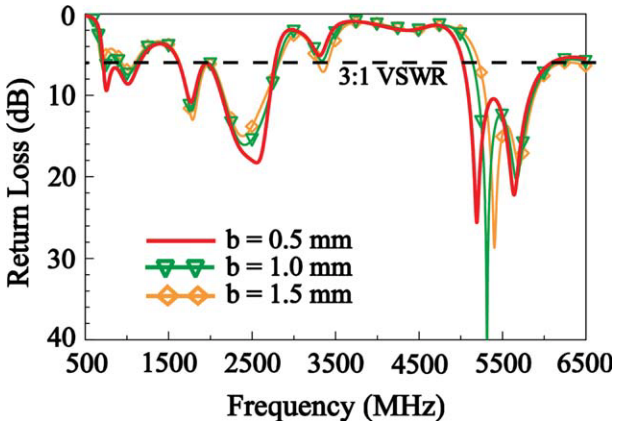

Figure 4 Simulated return loss for the proposed antenna as a function of the gap *b* between the shorting strip and the shorted monopole. Other dimensions are the same as given in Figure 1. [Color figure can be viewed in the online issue, which is available at wileyonlinelibrary.com]

wide bandwidth for the first band is still maintained; however, the third band is still not wide enough for the desired 5.2/5.8 GHz WLAN operation. By connecting a simple tuning stub to form Ref4, the impedance matching for the third band is improved. By modifying the simple tuning stub to be the tuning stub as shown in the proposed antenna, much improved impedance matching for frequencies over the third band is obtained, making the obtained 10-dB return loss bandwidth wide enough for the 5.2/5.8 GHz WLAN operation.

A parametric study for some major parameters in adjusting the impedance matching for frequencies over the three operating bands is also presented here. Figure 4 shows the simulated return loss for the proposed antenna as a function of the gap *b* between the shorting strip and the shorted monopole; other dimensions are the same as given in Figure 1. Results for the gap *b* varied from 0.5 to 1.5 mm are presented. Large effects on the impedance matching of the dual-resonance mode in the first band are seen. On the other hand, small effects on the second mode are observed. For the third band, the decrease in the gap *b* can also shift the lower-edge frequency of the third band to lower frequencies.

Figure 5 shows the simulated return loss for the proposed antenna as a function of the width *a* of the feeding strip. Results

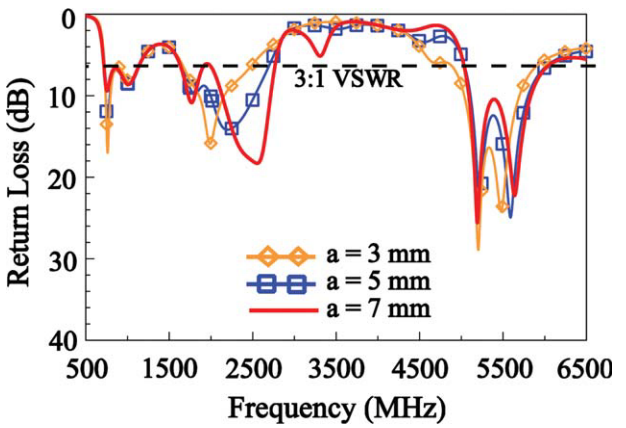

Figure 5 Simulated return loss for the proposed antenna as a function of the width *a* of the feeding strip. Other dimensions are the same as given in Figure 1. [Color figure can be viewed in the online issue, which is available at wileyonlinelibrary.com]

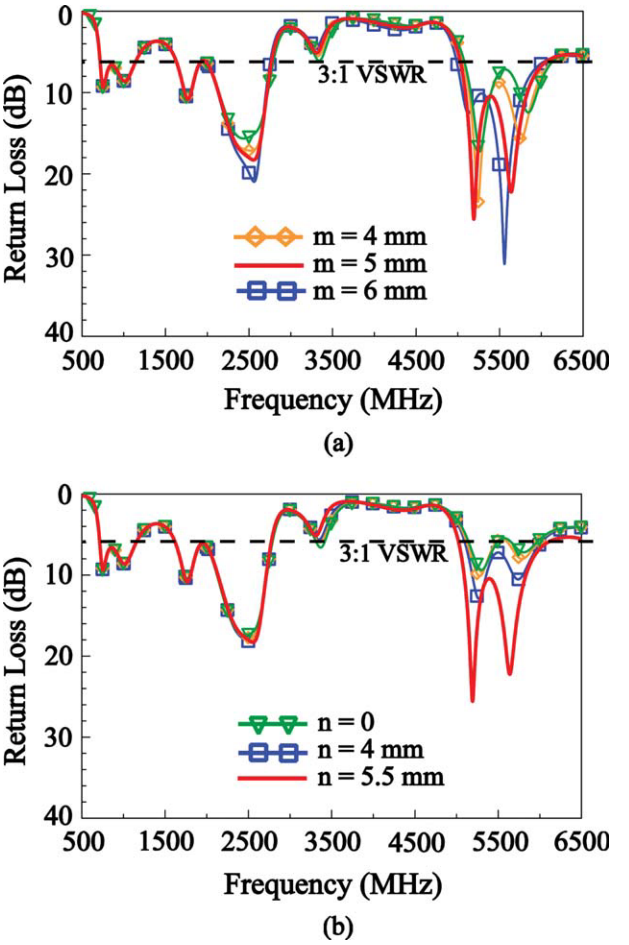

Figure 6 Simulated return loss for the proposed antenna as a function of (a) the length *m* and (b) the length *n* of the tuning stub connected to the shorting strip. Other dimensions are the same as given in Fig. 1. [Color figure can be viewed in the online issue, which is available at wileyonlinelibrary.com]

for the width *a* varied from 3 to 7 mm are presented. Large effects on the second band are seen, which confirms the discussion in Figure 3 that the widened feeding strip can achieve the desired wide second band. Also, small effects on the first and third bands are observed.

Figure 6 shows the simulated return loss for the proposed antenna as a function of the length *m* and *n* of the tuning stub connected to the shorting strip. Results for the length *m* varied from 4 to 6 mm are shown in Figure 6(a), while those for the length *n* varied from 0 to 5.5 mm are shown in Figure 6(b). For both cases, small effects on the first and second bands are observed. On the other hand, large effects on the third band are seen. This also confirms that the desired third band can be obtained by introducing the proposed tuning stub to the shorting strip.

Figure 7 shows the measured three-dimensional (3D) total-power radiation patterns for the proposed antenna. Four radiation patterns seen from four different directions of front, back, top, and bottom are shown. The radiation patterns at 830 MHz, which are typical for the frequencies in the first band, are similar to those of the traditional half-wavelength dipole antenna. At 1940 and 2450 MHz in the second band, more variations in the radiation patterns are seen; there are also dips or nulls seen in the azimuthal plane, the top direction, and the bottom direction of the radiation patterns. This characteristic indicates that the

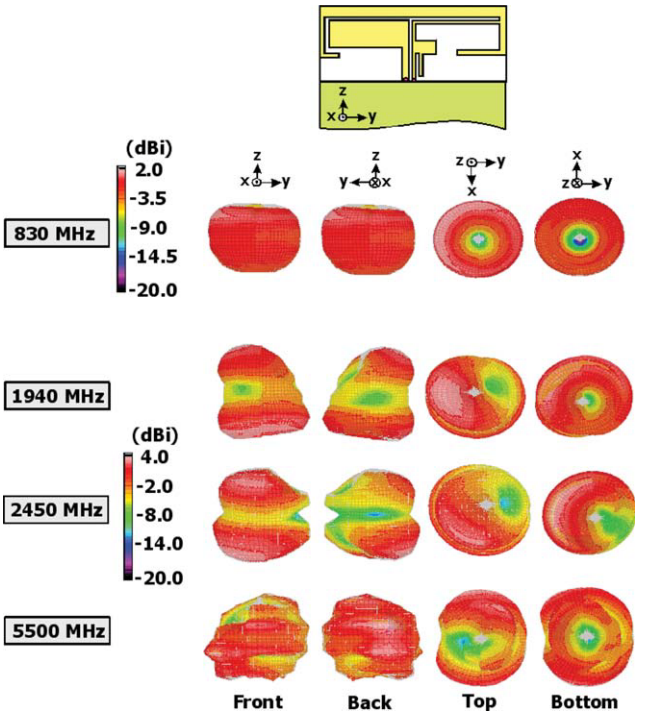

Figure 7 Measured three-dimensional (3D) total-power radiation patterns for the proposed antenna. [Color figure can be viewed in the online issue, which is available at wileyonlinelibrary.com]

excited resonant modes in the second band are related to the higher-order modes of the dipole antenna. At 5500 MHz in the third band, much more variations in the radiation patterns are seen; this is largely because that in this case, the system ground plane has dimensions much larger than the wavelengths of the operating frequencies and thus functions more like a reflector than a part of the radiator as in the first and second bands.

The measured radiation efficiency for the proposed antenna is presented in Figure 8. Results for the first and second bands are shown in Figure 8(a), while those for the third band are shown in Figure 8(b). The radiation frequencies are about 51–75%, 68–93%, and 67–92% for the first, second and third bands, respectively. The radiation frequencies are all better than 50% over the 11 operating bands, which are acceptable for practical mobile phone applications.

The SAR results are analyzed in Figure 9. In the figure, the SAR simulation model provided by SEMCAD version 14 [26] is shown, and the simulated 1-g SAR values for the two cases of the head only and the head and hand are also given. Results for the central frequencies of the eight operating bands of the LTE and WWAN are shown, and the impedance matching level at the testing frequency for the two cases is also provided. Notice that the proposed antenna is mounted at the bottom of the mobile phone, which has been shown to be promising to achieve decreased SAR values for the mobile phone [12, 19, 27–29]. The grip of the hand phantom on the mobile phone is shown in the figure, and the distance between the palm center and the plastic housing is set to 25 mm. These settings are reasonable for testing the SAR values with the user's hand presence [19]. In this study, the SAR results are tested using input power of 24 dBm for the GSM850/900 operation (859, 925 MHz), and 21 dBm for the GSM1800/1900 operation (1795, 1920 MHz), UMTS operation (2045 MHz) and LTE operation (740, 2350, 2595 MHz). For the head only case, the obtained 1-g SAR val-

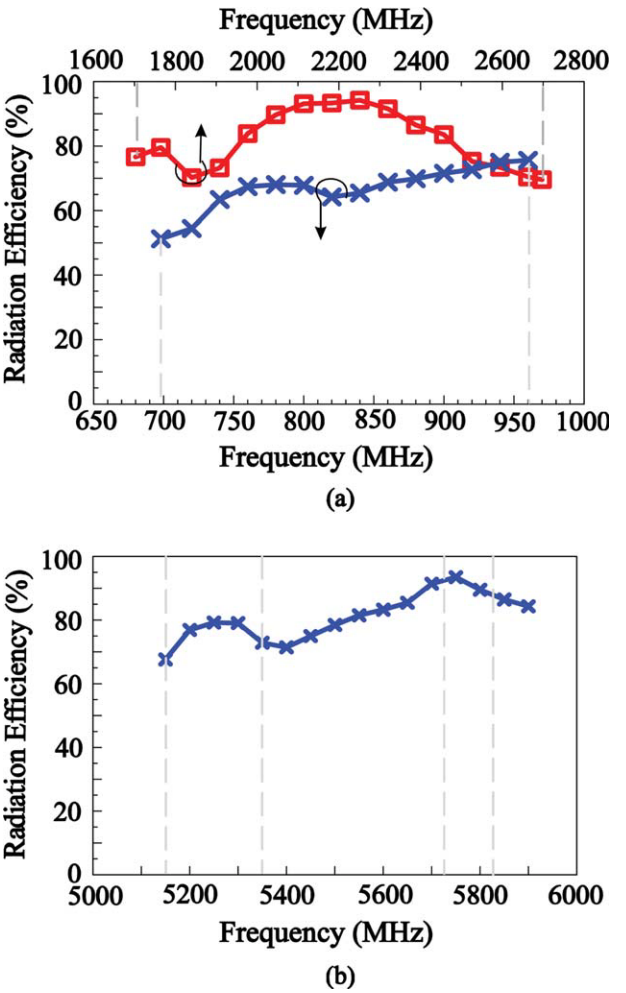

Figure 8 Measured radiation efficiency for the proposed antenna. (a) The first and second operating bands. (b) The third operating band. [Color figure can be viewed in the online issue, which is available at wileyonlinelibrary.com]

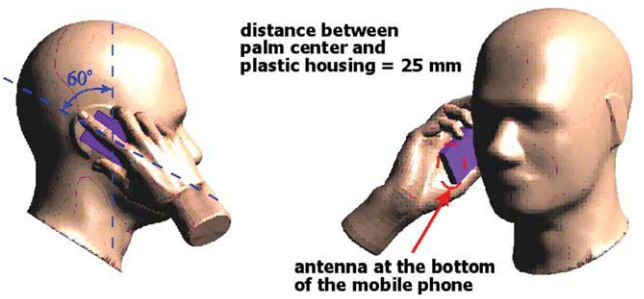

Frequency (MHz)		740	859	925	1795	1920	2045	2350	2595
1-g SAR (W/kg)	head only	0.57	1.18	1.42	0.81	0.21	0.29	0.96	1.01
	head and hand	0.57	1.29	1.58	1.08	0.73	0.74	1.69	2.45
Return loss (dB)	head only	9.7	6.1	7.2	11.6	7.5	7.7	17.4	18.0
	head and hand	9.5	5.6	7.0	13.4	7.6	8.4	14.1	13.9

Figure 9 SAR simulation model and the simulated 1-g SAR values for the proposed antenna. The return loss given in the table is the impedance matching level at the testing frequency. [Color figure can be viewed in the online issue, which is available at wileyonlinelibrary.com]

ues are all well below the limit of 1.6 W/kg [17]. For the head and hand case, small SAR increases at lower frequencies are seen as compared to those for the head only case. However, large SAR increases at higher frequencies are observed. At 2350 and 2595 MHz, the obtained SAR values are larger than the 1.6 W/kg limit. This behavior needs to be considered when the user's hand is included in the SAR specifications for the internal mobile pone antennas [19].

4. CONCLUSION

An internal mobile phone antenna suitable to be disposed on a small board space (600 mm^2 only) of the system circuit board and capable of providing three wide operating bands for the 11-band LTE/WWAN/WLAN operation has been proposed, fabricated, and studied. Detailed operating principle of the proposed antenna has been analyzed, and results for the fabricated antenna have been presented and studied. Good radiation characteristics for frequencies over the 11 operating bands have been observed. The obtained 1-g SAR results for the head-only case are also well below the 1.6 W/kg limit; this suggests that the proposed antenna is promising for practical mobile phone applications. However, when the user's hand holding the mobile phone is included in the testing, the obtained SAR results at higher frequencies in the LTE2300/2500 bands quickly increase and can no longer meet the 1.6 W/kg limit. This behavior requires further studies, especially when the user's hand holding the mobile phone is required to be included in the SAR testing in the near future [19].

REFERENCES

1. K.L. Wong, Planar antennas for wireless communications, Wiley, New York, 2003.
2. C.L. Tang and S.C. Lai, Multi-function IC antenna design and fabrication, In: Proceedings of the Asia-Pacific Microwave Conference, Singapore, 2009, Session TU4A, Paper no. 1741.
3. H. Rhyu, J. Byun, F.J. Harakiewicz, M.J. Park, K. Jung, D. Kim, N. Kim, T. Kim, and B. Lee, Multi-band hybrid antenna for ultra-thin mobile phone applications, Electron Lett 45 (2009), 773–334.
4. R.A. Bhatti, Y.T. Im, J.H. Choi, T.D. Manh, and S.O. Park, Ultra-thin planar inverted-F antenna for multistandard handsets, Microwave Opt Technol Lett 50 (2008), 2894–2897.
5. K.L. Wong, Y.C. Lin, and B. Chen, Internal patch antenna with a thin air-layer substrate for GSM/DCS operation in a PDA phone, IEEE Trans Antennas Propagat 55 (2007), 1165–1172.
6. K.L. Wong, Y.C. Lin, and T.C. Tseng, Thin internal GSM/DCS patch antenna for a portable mobile terminal, IEEE Trans Antennas Propagat 54 (2006), 238–242.
7. C.I. Lin and K.L. Wong, Printed monopole slot antenna for internal multiband mobile phone antenna, IEEE Trans Antennas Propagat 55 (2007), 3690–3697.
8. C.T. Lee and K.L. Wong, Uniplanar coupled-fed printed PIFA for WWAN/WLAN operation in the mobile phone, Microwave Opt Technol Lett 51 (2009), 1250–1257.
9. K.L. Wong and T.W. Kang, GSM850/900/1800/1900/UMTS printed monopole antenna for mobile phone application, Microwave Opt Technol Lett 50 (2008), 3192–3198.
10. T.W. Kang and K.L. Wong, Chip-inductor-embedded small-size printed strip monopole for WWAN operation in the mobile phone, Microwave Opt Technol Lett 51 (2009), 966–971.
11. C.H. Chang and K.L. Wong, Small-size printed monopole with a printed distributed inductor for penta-band WWAN mobile phone application, Microwave Opt Technol Lett 51 (2009), 2903–2908.
12. C.H. Chang and K.L. Wong, Printed lambda/8-PIFA for penta-band WWAN operation in the mobile phone, IEEE Trans Antennas Propagat 57 (2009), 1373–1381.
13. K.L. Wong and W.Y. Chen, Small-size printed loop antenna for penta-band thin-profile mobile phone application, Microwave Opt Technol Lett 51 (2009), 1512–1517.
14. W.Y. Chen and K.L. Wong, Small-size coupled-fed shorted T-monopole for internal WWAN antenna in the slim mobile phone, Microwave Opt Technol Lett 52 (2010), 257–262.
15. S. Sesia, I. Toufik, and M. Baker (Eds.), LTE, The UMTS long term evolution: From theory to practice, Wiley, New York, 2009.
16. C.T. Lee and K.L. Wong, Planar monopole with a coupling feed and an inductive shorting strip for LTE/GSM/UMTS operation in the mobile phone, IEEE Trans Antennas Propagat, in press.
17. American National Standards Institute (ANSI), Safety levels with respect to human exposure to radio-frequency electromagnetic field, 3 kHz to 300 GHz, ANSI/IEEE standard C95.1, April 1999.
18. J.C. Lin, Specific absorption rates induced in head tissues by microwave radiation from cell phones, Microwave (2001), 22–25.
19. C.H. Li, E. Ofli, N. Chavannes, and N. Kuster, Effects of hand phantom on mobile phone antenna performance, IEEE Trans Antennas Propagat 57 (2009), 2763–2770.
20. K.L. Wong and C.H. Huang, Bandwidth-enhanced internal PIFA with a coupling feed for quad-band operation in the mobile phone, Microwave Opt Technol Lett 50 (2008), 683–687.
21. C.H. Chang and K.L. Wong, Internal coupled-fed shorted monopole antenna for GSM850/900/1800/1900/UMTS operation in the laptop computer, IEEE Trans Antennas Propagat 56 (2008), 3600–3604.
22. C.H. Chang, K.L. Wong, and J.S. Row, Coupled-fed small-size PIFA for penta-band folder-type mobile phone application, Microwave Opt Technol Lett 51 (2009), 18–23.
23. K.L. Wong and S.J. Liao, Uniplanar coupled-fed printed PIFA for WWAN operation in the laptop computer, Microwave Opt Technol Lett 51 (2009), 549–554.
24. C.T. Lee and K.L. Wong, Uniplanar coupled-fed printed PIFA for WWAN/WLAN operation in the mobile phone, Microwave Opt Technol Lett 51 (2009), 1250–1257.
25. Ansoft Corporation HFSS, Available at http://www.ansoft.com/products/hf/hfss/.
26. SEMCAD, Schmid and Partner Engineering AG (SPEAG), Available at http://www.semcad.com.
27. Y.W. Chi and K.L. Wong, Quarter-wavelength printed loop antenna with an internal printed matching circuit for GSM/DCS/PCS/UMTS operation in the mobile phone, IEEE Trans Antennas Propagat 57 (2009), 2541–2547.
28. M.R. Hsu and K.L. Wong, Seven-band folded-loop chip antenna for WWAN/WLAN/WiMAX operation in the mobile phone, Microwave Opt Technol Lett 51 (2009), 543–549.
29. C.T. Lee and K.L. Wong, Internal WWAN clamshell mobile phone antenna using a current trap for reduced groundplane effects, IEEE Trans Antennas Propagat 57 (2009), 3303–3308.

FORWARD AND BACKWARD PERIODIC MICROSTRIP ANTENNA WITH A SLOTTED GROUND PLANE

Yuanxin Li,[1] Quan Xue,[2] and Yunliang Long[1]
[1] Department of Electronic Communications Engineering, Sun Yat-Sen University, Guangzhou, China 510275; Corresponding author: lipbzn@yahoo.com.cn
[2] State Key Laboratory of Millimeter Waves, City University of Hong Kong, Kowloon, Hong Kong

Received 14 February 2010

ABSTRACT: *A novel forward and backward periodic microstrip antenna is presented and tested in this article. The experimental results show that the main lobe scans electronically from 140° to 30° in* y–z *plane when the operating frequency increases from 3.2 to 8 GHz. The*